南京航空航天大学

论文集

（二〇〇六年）第26册

材料科学与技术学院

（第2分册）

南京航空航天大学科技部编

二〇〇七年三月

材料科学与技术学院

中

序号	姓 名	职 称	单 位	论 文 题 目	刊物.会议名称	年、卷、期	类别
71	顾冬冬 沈以赴	助 教 副教授	061 061	Development and characterisation of direct laser sintering multicomponent Cu based metal powder	Powder Metallurgy	2006.49.3 258-264	
72	顾冬冬 沈以赴	助 教 副教授	061 061	Selective Laser Sintering of Multi-component Cu-based Alloy for Creating Three-dimensional Metal Parts	Key Engineering Materials	2006. 315-316: 344-347	
73	顾冬冬 沈以赴 杨家林 王 洋	助 教 副教授 工程师 研究员	061 061 外单位 外单位	Effects of processing parameters on direct laser sintering of multicomponent Cu based metal powder	Materials Science and Technology	2006. 22.12 1449-1455	
74	顾冬冬 沈以赴 代 鹏 杨明川	助 教 副教授 本 科 研究员	061 061 外单位 外单位	Microstructure and property of sub-micro WC-10 %Co particulate reinforced Cu matrix composites prepared by selective laser sintering	Transaction of Nonferrous Metals Society of China	2006. 16 357-362	
75	顾冬冬 沈以赴	助 教 副教授	061 061	选区激光烧结 WC-10%Co 颗粒增强 Cu 基复合材料的显微组织	稀有金属材料与工程	2006.35 276-279	
76	顾冬冬 沈以赴	助 教 副教授	061 061	铜基金属粉末直接激光烧结工艺及成形件显微组织研究	中国机械工程	2006.17.20 2171-2175	
77	顾冬冬 沈以赴	助 教 副教授	061 061	磷元素对铜基金属粉末选区激光烧结作用机理	中国有色金属学报	2006.16.6 999-1005	
78	刘仕福 沈以赴 王少刚 王 蕾	硕 士 副教授 副教授 工程师	061 061 061 061	石墨表面钛金属化界面的组织及机理	稀有金属材料与工程	2006.35.7 1085-1088	
79	朱永兵 沈以赴	硕 士 副教授	061 061	钨铜纳米复合粉末的制备技术研究	金属功能材料	2006 .13.5 31-35	
80	徐 杰 刘子利 沈以赴 刘仕福	硕 士 副教授 副教授 硕 士	061 061 061 061	AZ31 镁合金 A - TIG 焊的研究	宇航材料工艺	2006.6 42-45	
81	姚正军 黄 斌 李 超 汤嘉立	正 高 硕 士 硕 士 硕 士	061 061 061 061	基于积件思想的材料热加工网络实验教学系统的研制	实验室研究与探索	2006 .25.1	

序号	姓 名	职 称	单 位	论 文 题 目	刊物.会议名称	年、卷、期	类别
82	张 静 姚正军 邱 宁	硕 士 正 高 硕 士	061 061 061	回收汽车用废旧塑料制备复合板材的力学性能	材料科学与工程学报	2006. 24. 3	
83	汤嘉立 姚正军 黄 斌 王红杰	硕 士 正 高 硕 士 硕 士	061 061 061 061	基于VB和VRML的虚拟仿真实验系统	计算机工程与设计	200627. 12	
84	邱 宁 姚正军 向建华 史有森	硕 士 正 高 正 高 副 高	061 061 外单位 外单位	热处理清洗含油废水的试验研究	金属热处理	2006.31.7	
85	邹 戈 姚正军	硕 士 正 高	061 061	微型注塑机机械部分的改进设计	江苏冶金	200.34. 6	
86	沈 凯 B.J.Duggan	讲 师 正 高	061 外单位	冷轧体心立方金属中微带的形成机制	南京理工大学学报	2006.30.5	
87	沈 凯 尹志民 王 涛	讲 师 正 高 正 高	061 外单位 外单位	时效处理状态下 7055 铝合金的微观结构演变	南京航空航天大学学报	2007.39.1	
88	沈 凯 B.J.Duggan	讲 师 正 高	061 外单位	Microbands and crystal orientation metastability in cold rolled interstitial-free steel	Acta Materialia	2007.55	
89	温建萍 程文孔 俞 娜	副教授 本 科 本 科	061 061 061	铝一塑自润滑材料的结构分析设计与摩擦磨损性能	中国机械工程	2006.17.21	
90	温建萍 李博明 温 涛 冯庆伟	副教授 高 工 工程师 工程师	061 外单位 外单位 外单位	油田回注污水对常用管线钢的腐蚀性	腐蚀科学与防护技术	2006.18.1	
91	甄明晖 温建萍 程文孔 李云仲	硕 士 副教授 本 科 本 科	061 061 061 061	PTFE/7075 铝合金镶嵌型自润滑材料的摩擦学行为	机械工程材料	2006.30.10	
92	甄明晖 温建萍 李云仲 俞 娜	硕 士 副教授 本 科 本 科	061 061 061 061	纳米蒙脱石填充 PTFE 和 UHMWPE 的摩擦磨损性能	材料科学与工程学报	2006.24.3	
93	张 翔 李子全	硕 士 教 授	061 061	RE、Mg 及 Ti 对 Zn-4.5%Al 合金耐蚀性的影响	材料开发与应用	2006.21.1	

序号	姓 名	职 称	单 位	论 文 题 目	刊物.会议名称	年、卷、期	类别
94	李子全 欧阳密 杨继年	教 授 硕 士 博 士	061 061 061	共混物对二次发泡聚丙烯的发泡效果和力学性能的影响	南京航空航天大学学报	2006.38.3	
95	李子全 常春荣 徐芸芸	教 授 硕 士 硕 士	061 061 061	退火对 ZnO 薄膜光吸收性能的影响	压电与声光	2006.28.5	
96	郑天航 李子全 陈健康 沈 凯 孙科沸	硕 士 教 授 高 工 讲 师 硕 士	061 061 061 061 061	Transitions of microstructure and photoluminescence properties of the terrace Ge/ZnO multilayers in certain annealing temperature region	Applied Surface Science	2006.252	
97	常春荣 李子全 徐芸芸	硕 士 教 授 硕 士	061 061 061	退火对溅射 ZnO 薄膜的形貌和内应力的影响	功能材料与器件学报	2006.12.2	
98	常春荣 李子全 徐芸芸 周衡志 骆心仪	硕 士 教 授 硕 士 博 士 副教授	061 061 061 061 061	间歇溅射和分段冷却对 ZnO 薄膜结构的影响	电子元件与材料	2006.25.5	
99	常春荣 李子全 徐芸芸	硕 士 教 授 硕 士	061 061 061	Sb_2O_3 掺杂对 ZnO 薄膜结构和光吸收性能的影响	光电子激光	2006.17.1	
100	周衡志 李子全 王 玲 杨玉岭 李祖泽	博 士 教 授 高 工 硕 士 硕 士	061 061 062 061 061	表面活性剂 Span80 和促进剂对 TiO_2/硅油电流变液性能的影响	材料工程	2006.4	
101	杨宝亮 陈 可 李子全	硕 士 博 士 教 授	061 061 061	电磁搅拌对富 Ce 混合稀土合金化 AZ91D 组织结构的影响	材料开发与应用	2006.21.1	
102	胡孝昀 郑明波 赵燕飞 刘劲松 李子全 曹洁明	工程师 博 士 博 士 博 士 教 授 副教授	061 062 062 061 061 062	利用胶体碳球为模板制备 SiO_2、TiO_2、SnO_2 空心球	化学研究与应用	2006.18.4	
103	李子全 周衡志	教 授 博 士	061 061	Aging microstructural characteristics of ZA-27 alloy and SiCp/ZA-27 composite	TRANSACTIONS OF NONFERROUS METALS SOCIETY OF CHINA	2006.16	

序号	姓 名	职 称	单 位	论 文 题 目	刊物.会议名称	年、卷、期	类别
104	胡孝昀 李子全 史长根	工程师 教 授 博士后	061 061 061	高温存贮对 SnAgCu/Cu 表面贴装焊点抗剪强度与显微组织的影响	焊接	2006.3	
105	潘 蕾 陶 杰 吴申庆 陈 峰 刘子利 陈照峰	副教授 教 授 教 授 教 授 副教授 副教授	061 061 外单位 外单位 061 061	原位反应烧结块的高能超声稀释过程分析	.复合材料学报	2005.12.6	
106	潘 蕾 陶 杰 吴申庆 陈 峰 刘子利	副教授 教 授 教 授 教 授 副教授	061 061 外单位 外单位 061	高能超声作用下两种锌基复合材料的制备与研究.	铸造	2005.12.54	
107	潘 蕾 陶 杰 刘子利 陈照峰	副教授 教 授 副教授 副教授	061 061 061 061	超声复合法制备的 SiC/ZA27 复合材料的力学性能.	南京航空航天大学学报	2005.37.5	
108	潘 蕾 陶 杰 陈照峰 刘子利	副教授 教 授 副教授 副教授	061 061 061 061	高能超声在颗粒/金属熔体体系中的声学效应	材料工程	2006.1	
109	王 芹 翁履谦 王秀华 杨文涛 台国安 王 函	中 级 教 授 硕 士 硕 士 硕 士 硕 士	061 061 061 061 061 061	活动注汽管线卡瓦在双头和螺栓断裂分析	全面腐蚀控制	2006.20.5	
110	王少刚 徐九华 姜澄宇	副教授 教 授 教 授	061 050 外单位	颗粒增强铝基复合材料焊接技术的发展	机械工程材料	2006.30.5	
111	王少刚 徐九华 姜澄宇	副教授 教 授 教 授	061 050 外单位	铝基复合材料焊接中的若干技术问题	宇航材料工艺	2006.00.4	
112	骆心怡 左敦稳 王 珉 李顺林 杨文涛 常 华	副教授 教 授 教 授 教 授 硕 士 硕 士	061 061 061 061 061 061	纳米 CeO_2/Zn 复合粉末的高能球磨法制备与表征	南京航空航天大学学报	2006.38.3 383－387	

序号	姓 名	职 称	单 位	论 文 题 目	刊物.会议名称	年、卷、期	类别
113	常　华 骆心怡 李顺林 杨文涛	硕　士 副教授 教　授 硕　士	061 061 061 061	高能球磨纳米 CeO_2/Zn 复合粉末的热压烧结	材料工程	2006.7 35－38	
114	刘仁培 董祖珏 潘永明	正　高 正　高 正　高	061 外单位 外单位	Solidification Crack Susceptibility of Aluminum Alloy Weld Metals	Transactions of Nonferrous Metals Society of China.	2006.16.1 110-116	
115	魏艳红	正　高	061	computer aided welding procedure qualification --- possibility, method and prospect	Proceedings of international symposium on computer-aided welding engineering, 19-22 October, Jinan, China	2006. 74-79	
116	董志波 魏艳红	博　士 正　高	外单位 061	Three dimensional modeling welding solidification cracks in multipass welding	Theoretical and AppliedFracture Mechanics	2006.46 156-165	
117	董志波 魏艳红 徐艳利	博　士 正　高 博　士	外单位 061 外单位	Predicting weld solidification cracks in multipass welds of SUS310 stainless steel	Computational materials science	2006.38: 459-466	
118	郑　勇 赵兴中 雷　文 汪胜祥	正　高 正　高 博　士 博　士	061 外单位 外单位 外单位	Effect of Bi_2O_3 addition on the microstructure and microwave dielectric characteristics of $Ba_{6-3x}(Sm_{0.2}Nd_{0.8})_{8+2x}Ti_{18}O_{54}$(x =2/3)ceramics	Materials Letters	2006.60. 459-463	
119	于海军 郑　勇 卜海建 严永林	硕　士 正　高 博　士 硕　士	061 061 061 061	热等静压处理对 Ti(C,N)基金属陶瓷组织和性能的影响	硬质合金	2006.23.3	
120	石增敏 郑　勇 刘文俊 袁　泉	中　级 正　高 博　士 中　级	外单位 061 外单位 外单位	Ti(C,N)基金属陶瓷刀具的切削性能	中国有色金属学报	2006.16.5	
121	刘文俊 熊惟皓 郑　勇	博　士 正　高 正　高	外单位 外单位 061	Ti(C,N)基金属陶瓷断口形貌及增韧机理	中国有色金属学报	2006.16.5	
122	汪　涛 张俊善	正　高 正　高	061 外单位	Thermoanalytical and metallographical investigations on the synthesis of TiAl3 from elementary powders	Materials Chemistry and Physics	2006. 99. 20	

序号	姓 名	职 称	单 位	论 文 题 目	刊物.会议名称	年、卷、期	类别
123	刘子利 刘希琴 徐 江 郭华明 潘青林 周海涛	副教授 副教授 副教授 硕 士 教 授 教 授	061 063 061 061 外单位 外单位	Effect of vacuum on the solidification process and microstructure of LFC magnesium alloy	Trans. Nonferrous Met. Soc. China	2006，16，sp3	
124	沈鸿烈 鲁林峰 Isao Sakamoto, Masaki Koike, Yunosuke Makita	教 授 博 士 博 士 博 士 博 士	061 061 国外 国外 国外	Formation of β-$FeSi_2$ from Fe/Si Multilayers by Sputtering	Proceedings of 8th ICSICT, Shanghai, China	2006 年，p1022-1024	
125	沈鸿烈 鲁林峰 尹玉刚 Isao Sakamoto, Masaki Koike, Yunosuke Makita	教 授 博 士 硕 士 博 士 博 士 博 士	061 061 061 国外 国外 国外	多层膜法制备光电薄膜的研究	中国太阳能光伏进展	2006 年，第 691 页至 694 页	
126	陈照峰 朱秀荣 刘子利 潘 蕾 陶 杰	副教授 副教授 副教授 副教授 教 授	061 外单位 061 061 061	Microstructure and mullitization of aluminosilicate matrix in Nextel 720/aluminosilicate composites prepared by LPCVI at 550°C	Ceramics International,	2006.32.6 687-690	
127	陈照峰 李 敏 史仪凯	副教授 讲 师 教 授	061 外单位 外单位	Alumina-silica composite coatings on graphite by CVD at 550°C	Journal of coatings technology,	2006.3.3 231-235	
128	董伟峰 肖 军 李 勇	硕 士 教 授 副教授	061	2.5 维编织复合材料的有限元模型与实验验证	第十四届全国复合材料学术会议论文集	2006 838-842	
129	张旭坡 李 勇 高 峰 张 钟 张建宝 肖 军	硕 士 副教授 硕 士 硕 士 硕 士 教 授	061	M46J/BMP-316 复合材料缠绕制品热胀成型工艺研究	第十四届全国复合材料学术会议论文集	2006 477-482	

序号	姓 名	职 称	单 位	论 文 题 目	刊物.会议名称	年、卷、期	类别
130	张旭坡 李 勇 肖 军 邓智泉	硕 士 副教授 教 授 硕 士	061	磁悬浮电机转子加强环设计及工艺研究	宇航材料工艺	2006.34.4 33-37	
131	张旭坡 李 勇 肖 军 谭永刚 原永虎 龙国荣	硕 士 副教授 教 授 硕 士 硕 士 副 高	061 061 061 061 061 外单位	NY9200G 树脂热熔法预浸料制备复合材料工艺及性能研究	中国科技论文在线	2006 1-7	
132	缪 强 崔彩娥 潘俊德 段良辉 刘亚萍	教 授 副教授 教 授 硕 士 硕 士	061 外单位 外单位 外单位 外单位	Tribological Behavior of Magnesium Alloy AZ91 Coated with TiN/CrN by Arc-glow Plasa Depositing	Chinese Journal of Aeronautics	2006.19.3	
133	缪 强 崔彩娥 潘俊德 张平则	教 授 教 授 教 授 副教授	061 外单位 外单位 061	Improving wear resistance of magnesium alloy AZ91D by TiN-CrN multilayer coatings	Transaction of Nonferrous Metals Society of China	2006,16	
134	范吉阳 吴兴龙 李红霞 刘宏伟 G.G.Siu Paul K. Chu	讲 师 教 授 讲 师 讲 师 教 授 教 授	061 外单位 外单位 外单位 外单位 外单位	Luminescence from colloidal 3C-SiC nanocrystals in different solvents	Applied Physics Letters	2006.01	
135	张平则 徐 重 张高会 贺志勇	副教授 教 授 副教授 教 授	061 061 外单位 外单位	Plasma surface alloying of titanium alloy for enhancing burn-resistant property	Transaction of Nonferrous Metals Society of China	2006,16	
136	高明慧 王 玲 薛建军 吴永军	高 工 高 工 副教授 硕 士	062 062 062 062	无汞盐快速分光光度法与标准法测定水中 COD 值的比较	扬州大学学报	2006．00.02	
137	金丹萍 薛建军 迟长云	硕 士 副教授 硕 士	062 062 062	钛基炭电极处理回用水的实验研究	功能材料	2006..37.SUP 752~754	
138	雷 斌 薛建军 秦 亮 阮平平	硕 士 副教授 硕 士 硕 士	062 062 061	纳米管 TiO_2-Pt 修饰电极降解含酚类废水	功能材料	2006..37.SUP 744~746	

Development and characterisation of direct laser sintering multicomponent Cu based metal powder

D. D. Gu* and Y. F. Shen

Recent advances in direct metal laser sintering (DMLS) have improved this technique considerably; however, it still remains limited in terms of material versatility and controllability of laser processing. In the present work, a multicomponent Cu based metal powder, which consisted of a mixture of Cu, Cu–10Sn and Cu–8·4P powder, was developed for DMLS. Sound sintering activities and high densification response were obtained by optimising the powder characteristics and manipulating the processing conditions. Investigations on the microstructural evolution in the laser sintered powder show that liquid phase sintering with partial or complete melting of the binder (Cu–10Sn), but non-melting of the cores of structural metal (Cu) acts as the feasible mechanism of particle bonding. The additive phosphorus acts as a fluxing agent to protect the Cu particles from oxidation and shows a concentration along grain boundaries owing to the low solubility of P in Cu and the short thermal cycle of laser sintering. A directionally solidified microstructure consisting of significantly refined grains is formed, which may be ascribed to laser induced non-equilibrium effects such as high temperature gradient and rapid solidification.

Keywords: Direct metal laser sintering, Cu based metal powder, Microstructure

Introduction

Direct metal laser sintering (DMLS) is a newly developed material additive manufacturing process which enables the quick production of complex shaped three-dimensional (3D) parts directly from metal powder.[1] As compared with indirect laser sintering or other conventional processes, the main advantages associated with this technique are elimination of cost and time consuming preprocessing and post-processing steps.[2,3] In other words, the purpose of DMLS is to fabricate functional metallic parts in a single process. Therefore, the DMLS process is regarded as 'rapid manufacturing' more than 'rapid prototyping'.[4]

So far, there exist abundant research reports in the area of DMLS. Recent works mainly focus on the direct laser sintering of the prealloyed metal powder (e.g. alloy 625,[2] Ti–6Al–4V,[5] bronze,[6] stainless steel,[7] high speed steel,[8] low carbon steel[9] and tool steel[10]) and the multicomponent metal powder (e.g. bronze–Ni–CuP,[11] Ni-alloy–Cu,[12] Cu–SCuP,[3,13] iron–graphite,[1,14] Fe–C–Cu–Mo–Ni[15] and Fe–Cu–W[16]). Most investigations have been carried out on developing the workable materials and exploring the fundamentals of laser processing. Although recent advances in DMLS have improved this technique considerably, it still remains limited in terms of material versatility and sintering quality.[17] Only a few metallic materials have been commercialised, which limits the industrial application of DMLS. Common problems associated with DMLS such as oxidation, balling and curling might result in a series of processing defects such as low sintered density, weak strength and high surface roughness.[18] In fact, DMLS is a complex metallurgical process exhibiting multiple modes of heat and mass transfer, and in some cases, chemical reactions.[1,19] Furthermore, these complex phenomena are strongly material dependant and governed by powder characteristics in terms of chemical constituents, particle shape, particle size and its distribution and loose packing density.[19,20] However, not much previous work has been reported on the basic principles of powder preparation and the microstructural evaluation of the laser processed materials.[21]

This paper presents the development and characterisation of a multicomponent Cu based metal powder for DMLS. The sintering behaviour, phase transformation and microstructural evolution during laser sintering of this powder system are also addressed.

Experimental procedure

Powder preparation

Electrolytic 99% purity Cu powder, water atomised CuSn (10 wt-%Sn) powder and gas atomised CuP (8·4 wt-%P) powder were used in this experiment. The as received powder was sieved through a series of mesh

College of Materials Science and Technology, Nanjing University of Aeronautics and Astronautics, 29 Yudao Street, Nanjing 210016, China

*Corresponding author, email dongdonggu@hotmail.com

Published by Maney on behalf of the Institute
Received 8 October 2005; accepted 28 December 2005
DOI 10.1179/174329006X95662

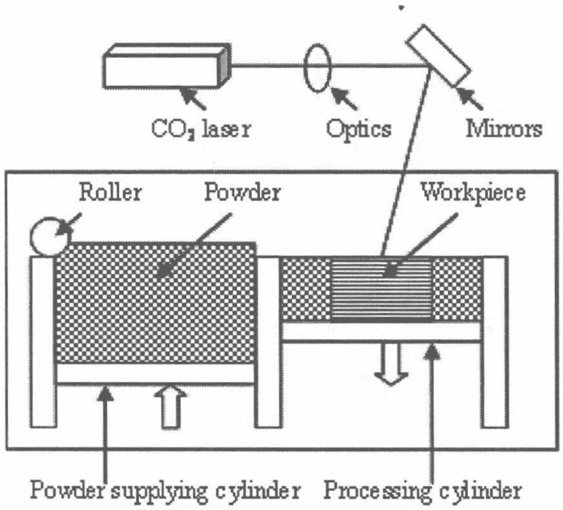

1 Schematic of DMLS apparatus

size to extract powder of desirable particle size. Size distribution of the particles was measured using a MS2000 laser particle size analyzer. The morphology of the starting powder was examined by a Quanta 200 scanning electron microscopy (SEM).

The three kinds of powder were mixed according to CuSn : Cu : CuP ratio of 30 : 60 : 10 by weight. Powder mixing was performed in a cylindrical vessel with a vacuum pumping system at the rotation velocity of 100 rev min^{-1} for 90 min.

Laser sintering process

A DMLS system developed at the China Academy of Engineering Physics (CAEP) was used for the laser sintering experiments. Figure 1 depicts a schematic diagram of the apparatus. The system consists of a continuous wave CO_2 (λ=10·6 μm) laser with a maximum output power of 2000 W, an automatic powder delivery system and a chamber with atmosphere control.

Single layer melting tests were firstly performed by repeated scanning a powder layer (0·3 mm in thickness) using a simple linear raster scan pattern. The laser processing parameters used were listed as follows: spot size of 0·30 mm, laser power of 200–500 W, scan speed of 0·01–0·06 m s^{-1} and scan line spacing of 0·15 mm. The entire sintering process was carried out in air at room temperature. From these experiments, several optimal processing parameters were chosen for further preparation of rectangular samples for microstructural investigations. Further details of the DMLS process can be found in the literatures.[1,15]

Characterisation

Samples for metallographic examination were prepared using standard techniques and etched with a mixture of $FeCl_3$ (5 g), HCl (10 mL) and distilled water (100 mL) for 30 s. Surface morphology and microstructure were characterised using the Quanta 200 SEM and a SPI3800 atomic force microscope (AFM). Chemical composition was examined by an EDAX spectroscopy. Phase identification was performed with a Bruker D8 Advance X-ray diffraction (XRD) analyser.

Results and discussion

Powder characteristics

The material system as investigated was mixed by three components: Cu powder, CuSn powder and CuP powder. The Cu powder with higher melting point of ~1083°C acts as the structural metal during laser sintering, while the prealloyed CuSn (10 wt-%Sn) with lower solidus temperature of ~840°C and liquidus one of ~1020°C acts as the binder. Phosphorus was added as prealloyed CuP (8·4 wt-%P) powder, taking as a fluxing agent to improve the wetting ability and thus aid in laser processing.

The specifications of particle size of the starting powder are listed in Table 1. It is clear that the powder system was mixed by coarse Cu powder and fine CuSn and CuP powder. Such bimodal mixture with a broad particle size distribution (>60 μm) may lead to an increase in the loose packing density than powder systems with a uniform particle size.[15] Generally, a powder system with a high loose packing density is preferred in the DMLS process.[20] In addition, the fine CuSn and CuP particles can provide larger surface area to absorb more laser energy, thereby increasing the particle temperature and the sintering kinetics.

Figure 2 shows the morphologies of the starting powder. The Cu powder exhibited an irregular and ligamental structure (Fig. 2*a*). The irregularly shaped Cu powder used may facilitate particle rearrangement during liquid phase sintering and thus assist densification, because the torques, which are formed owing to misalignment of the particles' centre, tend to rotate the particles in the liquid.[22] The CuSn powder showed an ellipsoidal shape (Fig. 2*b*), while the CuP powder exhibited a generally spherical morphology (Fig. 2*c*). Such spherical or near spherical particles in the powder system give higher coordination number and resultant higher loose packing density. Figure 2*d* shows that the fine particles were dispersed uniformly around the coarse particles after mixing. A homogenous powder blend with less agglomeration of the binder is of critical importance to increase the thermal absorption rate of the laser beam. Furthermore, a homogeneous dispersion of the binder can lead to a favourable rheological property of the solid–liquid system during sintering,[20] which further enhances wetting characteristics and accelerates particle rearrangement, hence permitting a high densification.

Mechanisms of particle bonding

Figure 3 depicts an overview on the change of mechanisms of single layer melting. Over the entire range of laser powers and scan speeds, five process regions as

Table 1 Specifications of particle size of starting powder

Powder	Size, μm	Volume fraction	Mean particle diameter, μm
Cu	28–75	20%<38 μm, 80%<65 μm	54
CuSn	11–46	20%<22 μm, 80%<40 μm	28
CuP	5–24	20%<9 μm, 80%<20 μm	16

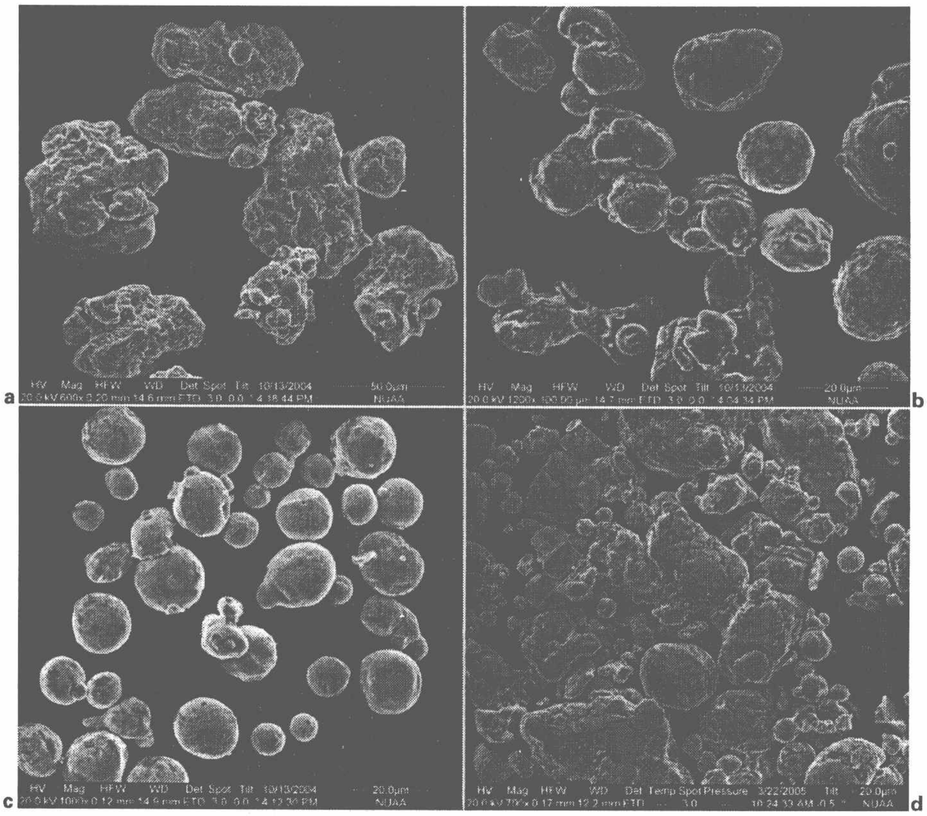

a **Cu powder;** ***b*** **CuSn powder;** ***c*** **CuP powder;** ***d*** **powder mixture**
2 Micrographs of starting metal powder (SEM)

follows are defined to characterise each single layer sample:

(i) slight melting: the energy delivered was insufficient to cause any significant melting of the binder, resulting in the formation of weak interparticle contacts through short necks
(ii) partial melting: the incident energy could generate sufficient liquid phase through the partial or complete melting of the binder, while the structural metal particles remained in solid. The solid particles were bonded together by the molten liquid to form a continuous network of relatively small agglomerates, leading to an almost fully dense sintered surface (Fig. 4*a*)

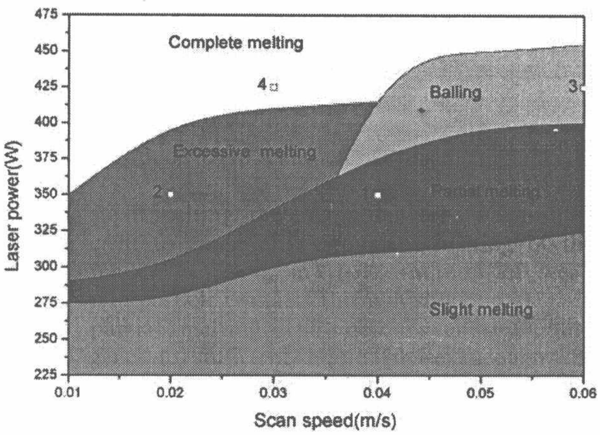

3 Single layer melting processed over wide range of laser powers and scan speeds

(iii) excessive melting: the laser sintering at a high laser power with a low scan speed resulted in the formation of excessive molten material because of the highly localised heat input and the greater heat affected zone around the laser beam. Under this condition, coarse columnar agglomerates were formed, between which open and deep pores were visible (Fig. 4*b*)
(iv) balling: at a high laser power with a high scan speed, a liquid scan track of cylindrical shape was generated, which in turn broke up to a row of spheres owing to surface energy reduction ('balling' effect). This resulted in the formation of significantly coarsened metallic agglomerates and large pores (Fig. 4*c*)
(v) complete melting: at an even higher laser power for all scan speeds, the incident energy was high enough to make complete melting of the powder occurred, producing a long thin melt pool. The liquid broke up at longer intervals owing to significant shrinkage during liquid–solid transition, thereby forming a porous surface consisting of highly rippled metal lumps (Fig. 4*d*). Furthermore, EDX analysis was detected the formation of severe non-metallic inclusions in this case as a consequence of oxidation.

Typical surface morphologies of the laser sintered powder obtained on the described regions are shown in Fig. 4.

A close look at the laser sintered surfaces (Fig. 4) demonstrates that liquid phase sintering with partial or complete melting of the binder, but non-melting of the cores of structural metal proves to be a feasible bonding

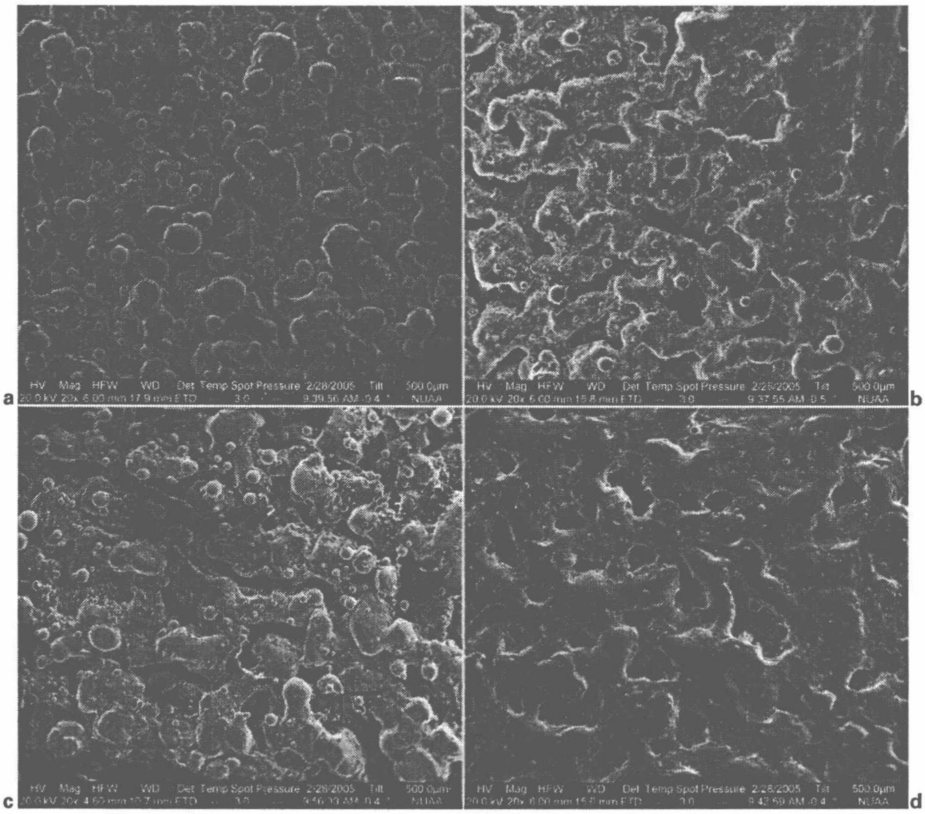

a 350 W, 0·04 m s^{-1} (point 1 in Fig. 3); *b* 350 W, 0·02 m s^{-1} (point 2); *c* 425 W, 0·06 m s^{-1} (point 3); *d* 425 W, 0·03 m s^{-1} (point 4)

4 Micrographs of surface morphologies of laser sintered samples at different laser power and scan speed combinations (SEM)

mechanism for this powder system. From the parameter dependence descriptions (Fig. 3), it can be noticed that the process window is quite narrow and the requirements for adjusting the laser processing parameters are critical: sintering can only be smoothly processed at temperatures exceeding the melting point of the binder, but below the melting point of the structural metal. With the suitable sintering mechanism permitted, a rectangular sample with dimensions of 100 × 10 × 30 mm was fabricated at a laser power of 350 W and a scan speed of 0·04 m s^{-1} (Fig. 5). From the images, it can be seen that the powder was smoothly sintered without any splash (Fig. 5*a*) and the laser sintered part showed very little dimensional deformation and balling phenomena (Fig 5*b*).

Structural analysis

Figure 6 shows typical XRD patterns of the powder mixture and the above laser sintered sample. The starting powder blend mainly consisted of a matrix metal Cu and an intermetallic compound $Cu_{41}Sn_{11}$, while Cu_3P acted as the primary eutectic constituent phase of the prealloyed CuP (Fig. 6*a*). After laser sintering, the diffraction peaks of the retained Cu decreased and slightly shifted to a low diffraction angle (Fig. 6*b*), resulting in an increase in the lattice parameters. This may be caused by the substitutional replacement of Cu atoms possessing smaller radii (0·128 nm) with Sn atoms possessing larger radii

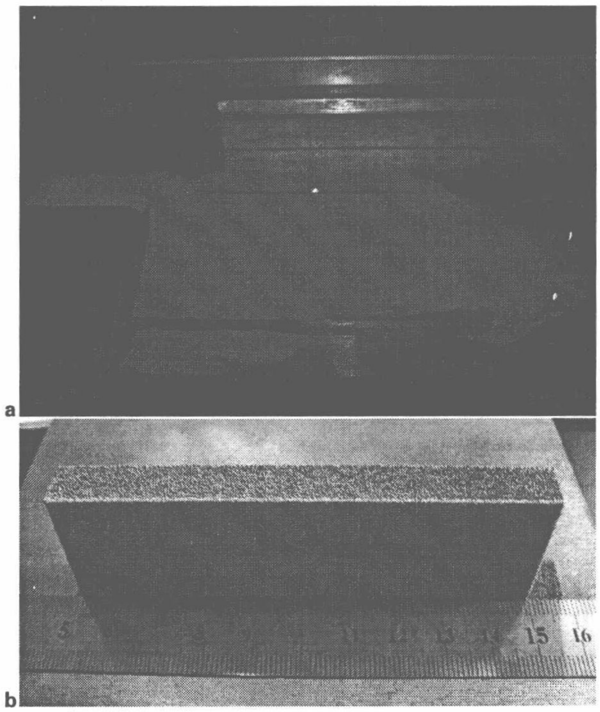

5 Photographs of *a* laser sintering process and *b* laser sintered sample

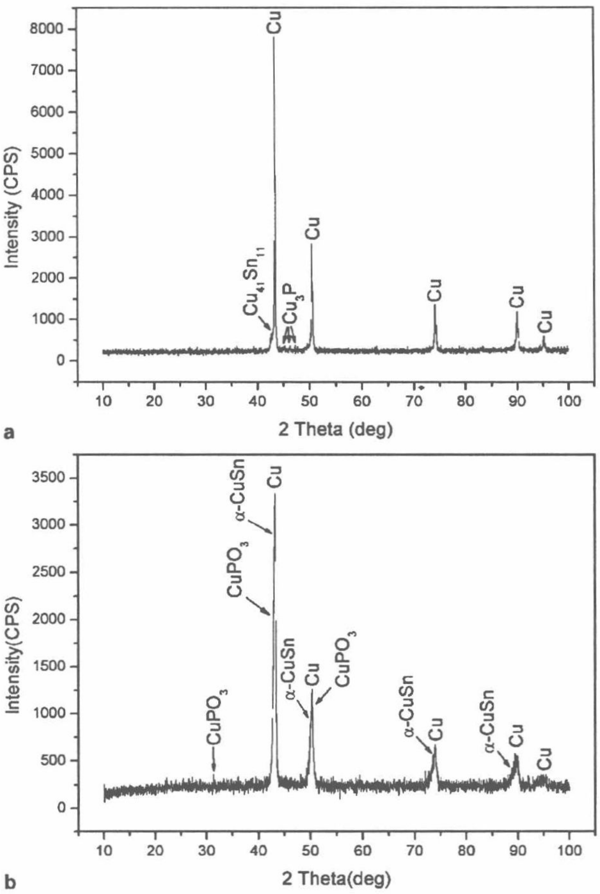

6 X-ray patterns of *a* starting powder blend and *b* laser sintered sample

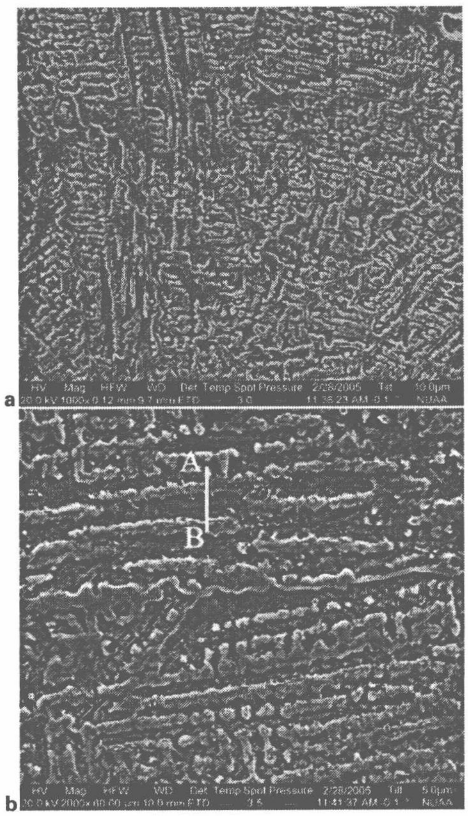

a ×1000; *b* ×2000

7 Typical microstructures of laser sintered sample at different magnifications

(0·158 nm). This analysis is further proved by detecting the formation of α-CuSn phase, a solid solution of Sn in Cu (Fig. 6*b*). In addition, Fig. 6*b* reveals the presence of phosphorus as $CuPO_3$, but without the existence of oxide CuO or Cu_2O. This may be because phosphorus acts as an *in situ* sink for oxygen during sintering, protecting the Cu particle surface from oxidation and permitting a sound solid–liquid wetting characteristics with minimal or no balling effect.

Microstructure

Figure 7 shows the characteristic microstructure of the laser sintered sample. It can be seen that a highly continuous network of dendrites was formed (Fig. 7*a*). The EDX results reveal that such dendrites were CuSn solid solution, while the areas between dendrites were identified to be Cu rich. This indicates that the mechanism of this process is liquid phase sintering, and the liquid formation is achieved by melting of CuSn but non-melting of the cores of Cu particles. Partial melting of the particles by laser irradiation may result in the formation of a so called 'sintering pool' containing a solid–liquid mixture, which differs from the melt pool with a single liquid phase formed in direct metal laser remelting (DMLR)[23] or selective laser melting (SLM)[24] process. Eventually, the sintering pool undergoes solidification by preferred nucleation of epitaxial grains off the surface of remained Cu solid particles. An EDX line scan was performed across the dendrites from position A to B (Fig. 7*b*), with the content distribution of Cu, P and Sn shown in Fig. 8. It is observed that the Cu generally demonstrated a higher content distribution. The P content at the boundaries of dendrites was much higher than that in other positions, while the Sn content showed a relatively slight change except for little higher concentration in the dendrites. This phenomenon can be explained with the following reasons. During laser sintering, the melting of the binder CuSn occurs because of the relatively higher absorption to laser energy and lower solidus temperature of ~840°C. At the melting temperature of the CuSn, the CuP powder is expected to be fully molten as it has a lower eutectic

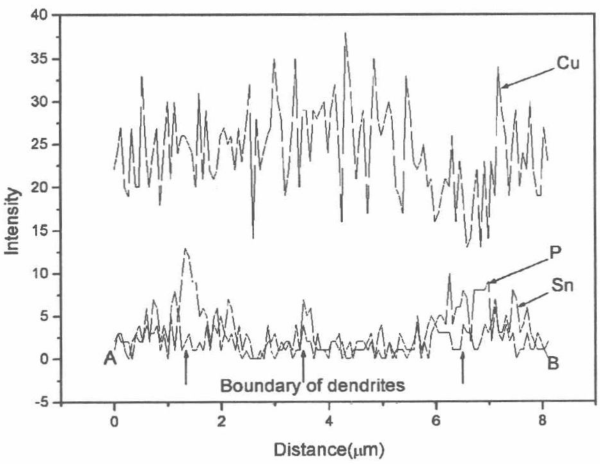

8 Distributions of Cu, P and Sn elements shown by EDX trace along AB line in Fig. 7*b*

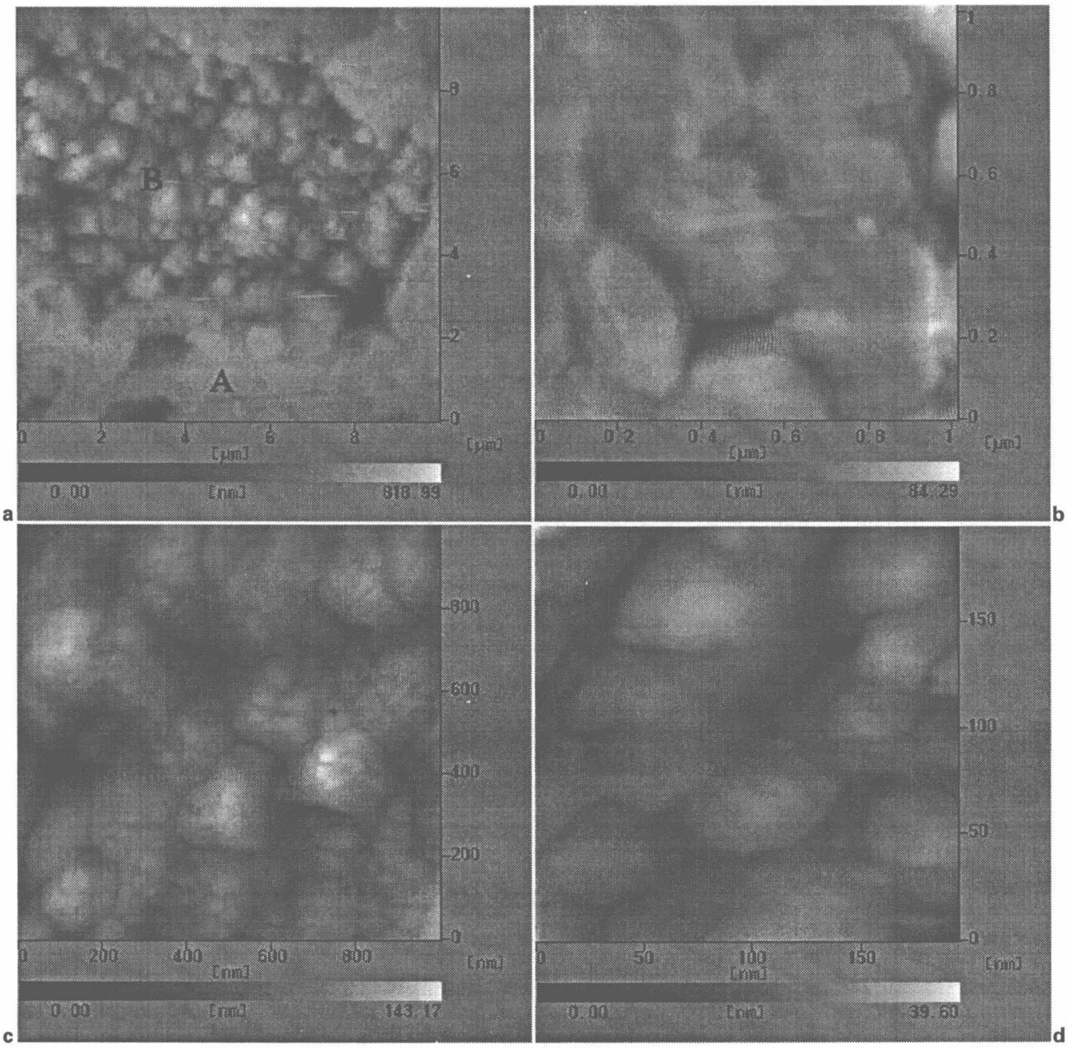

a 10×10 µm scan area; *b* 1×1 µm scan area on zone A; *c* 1×1 µm scan area on zone B; *d* 200×200 nm scan area on zone B

9 Images of AFM of ultrafine structures on microareas

temperature of ~714°C. The Cu particles, however, are dissolved slightly in the wetting liquid owing to a higher melting point of ~1083°C. With the laser beam moving away, the high temperature phase α-Cu starts to solidify. Owing to a relatively high solubility of Sn in Cu (~15 wt-% at 200°C),[25] the formation of the α-CuSn solid solution (Fig. 6*b*) as well as the precipitation in dendritic morphologies can occur (Fig. 7*a*). However, because of a low mutual solubility of P and Cu (<2 wt-% at 200°C)[25] and the rapid heating process, the solution of P in Cu may be significantly suppressed and the P tends to segregate along the boundaries of the solidified phase (Fig. 8).

Metallographic study at a higher magnification shows that the dendrites grew directionally along certain preferred but not changeless orientations (Fig. 7*b*). Because an extremely high temperature gradient exists in the sintering pool, the dendrites grow directionally along the heat flow direction; meanwhile, the preferred crystal orientation of the grains also shows pronounced influence on the direction of the growing dendrites.[26] Owing to the dynamic effects induced by the mobile laser scanning, the heat flow direction changes with the solid/liquid interface advancing. Thus, the dendrites may adjust their growth direction between heat flow direction and their preferred orientation. Furthermore, Fig. 7*b* reveals that the side branches of the dendrites were not well developed and the dendritic cellular structures were coexisted. This is attributed to the high temperature gradient and high solidification rate induced by laser scanning. Also, Fig. 7*b* shows that the primary dendritic spacing was generally <5 µm, from which it can be concluded that the temperature gradient and the solidification rate can reach $1\cdot0\times10^{6}$ km^{-1} and $6\cdot0\times10^{3}$ K min^{-1} respectively.[20,27]

Analysis of AFM performed on microscan areas shows the formation of ultrafine sintered structures (Fig. 9). It can be seen that the average grain size of the precipitated CuSn solid solution (zone A in Fig. 9*a*) was ~250 nm (Fig. 9*b*). Here, it should be noted that the high solidification rate and the large degrees of undercooling of alloys may lead to the refinement of the scale of microstructures. Interestingly, the results, shown in Fig. 9*c*, reveal that the grains of the remained Cu phase (zone B in Fig. 9*a*) were consisted of ultrafine nanometre scaled subgrains, with the mean grain size of ~50 nm (Fig. 9*d*). It is well known that the laser heating is a transient non-equilibrium process.[28] For high speed heating, thermal expansion will lag behind temperature, i.e. even though temperature reaches a maximum, the thermal expansion remains unfinished.[29] The non-synchronous change of temperature rise and thermal expansion leads to a high non-stationary thermal stress in the sintering system.[30] This will be beneficial in refinement of the microstructural scale of the copper phase, even though it has not been molten by the laser beam during sintering. The significant grain refinement in the sintered structures holds a great potential in improving the performance of the laser processed materials.

Conclusions

Based on the experiments conducted, conclusions can be drawn as follows:

1. A multicomponent Cu based metal powder is developed for direct laser sintering. The shape, size and its distribution of the particles as well as the dispersion homogeneity of the powder system influence sintering behaviour and densification response.

2. The direct laser sintering of this powder system is based on the mechanism of liquid phase sintering with partial or complete melting of the binder (CuSn), full melting of the additive (CuP) and non-melting of the cores of the structural metal (Cu).

3. With optimising the processing parameters such as laser power and scan speed, the workable sintering mechanism and sound interparticle bonding can be permitted.

4. Mutual solubility and reactivity between the different constitutes of the powder blend leads to the formation of new phases as well as solution and precipitation phenomena during short laser irritation.

5. The laser induced non-equilibrium effect significantly refines the grain size of the sintered structure.

Acknowledgements

The authors would like to thank the financial support from the Joint Fund of National Natural Science Foundation of China and China Academy of Engineering Physics (10276017), the Aeronautical Science Foundation of China (04H52061) and the Scientific Research Innovations Foundation of Nanjing University of Aeronautics and Astronautics (S0403-061). The authors also acknowledge Professor Y. Wang, Dr J. L. Yang and Dr X. F. Shen for their helps in preparation of the laser sintered samples. The helps of Dr Y. Jiang in the AFM investigation are also appreciated.

References

1. A. Simchi and H. Pohl: *Mater. Sci. Eng. A*, 2004, **A383**, 191–200.
2. S. Das, J. J. Beaman, M. Wohlert and D. L. Bourell: *Rapid Prototyping J.*, 1998, **4**, (3), 112–117.
3. H. H. Zhu, L. Lu and J. Y. H. Fuh: *Mater. Sci. Eng. A*, 2004, **A371**, 170–177.
4. Y. Tang, J. Y. H. Fuh, H. T. Loh, Y. S. Wong and L. Lu: *Mater. Design*, 2003, **24**, 623–629.
5. S. Das, M. Wohlert, J. J. Beaman and D. L. Bourell: *Mater. Design*, 1999, **20**, 115–121.
6. Y. A. Song: *Ann. CIRP*, 1997, **46**, (1), 127–130.
7. Z. Katz and P. E. S. Smith: *Proc. Inst. Mech. Eng. B: J. Eng. Manuf.*, 2001, **215**, (11), 1497–1504.
8. H. J. Niu and I. T. H. Chang: *J. Mater. Sci.*, 2000, **35**, 31–38.
9. A. N. Chatterjee, S. Kumar, P. Saha, P. K. Mishra and A. R. Choudhury: *J. Mater. Process. Technol.*, 2003, **136**, 151–157.
10. A. I. Kovalev, V. P. Mishina, D. L. Wainstein, V. I. Titov, V. F. Moiseev and N. K. Tolochko: *J. Mater. Eng. Perform.*, 2002, **11**, (5), 492–495.
11. M. W. Khaing, J. Y. H. Fuh and L. Lu: *J. Mater. Process. Technol.*, 2001, **113**, 269–272.
12. N. Tolochko, S. Mozzharov, T. Laoui and L. Froyen: *Rapid Prototyping J.*, 2003, **9**, (2), 68–78.
13. H. H. Zhu, L. Lu and J. Y. H. Fuh: *J. Mater. Process. Technol.*, 2003, **140**, 314–317.
14. K. Murali, A. N. Chatterjee, P. Saha, R. Palai, S. Kumar, S. K. Roy, P. K. Mishra and A. R. Choudhury: *J. Mater. Process. Technol.*, 2003, **136**, 179–185.
15. A. Simchi, F. Petzoldt and H. Pohl: *J. Mater. Process. Technol.*, 2003, **141**, 319–328.
16. H. H. Zhu, J. Y. H. Fuh and L. Lu: *Proc. Instn. Mech. Engrs., Part C: J. Mech. Eng. Sci.*, 2003, **217**, (1), 139–147.
17. P. Fischer, V. Romano, H. P. Weber, N. P. Karapatis, E. Boillat and R. Glardon: *Acta Mater.*, 2003, **51**, 1651–1662.
18. Y. Tang, H. T. Loh, Y. S. Wong, J. Y. H. Fuh, L. Lu and X. Wang: *J. Mater. Process. Technol.*, 2003, **140**, 368–372.
19. S. Das: *Adv. Eng. Mater.*, 2003, **5**, (10), 701–711.
20. A. Simchi, F. Petzoldt and H. Pohl: *Int. J. Powder Metall.*, 2001, **37**, (2), 49–61.
21. D. Uzunsoy, I. T. H. Chang and P. Bowen: *Powder Metall.*, 2002, **45**, (3), 251–254.
22. H. J. Niu and I. T. H. Chang: *Scr. Mater.*, 1999, **41**, (1), 25–30.
23. R. Morgan, C. J. Sutcliffe and W. O'neill: *J. Mater. Sci.*, 2004, **39**, 1195–1205.
24. J. P. Kruth, L. Froyen, J. Van vaerenbergh, P. Mercelis, M. Rombouts and B. Lauwers: *J. Mater. Process. Technol.*, 2004, **149**, 616–622.
25. M. Hansen and K. Anderko: 'Constitution of binary alloys', 2nd edn; 1958, New York, McGraw-Hill.
26. Q. Y. Pan, X. Lin, W. D. Huang, Y. H. Zhou and G. L. Zhang: *Mater. Res. Bull.*, 1998, **33**, (11), 1621–1633.
27. Q. Y. Pan, W. D. Huang, Y. M. Li, X. Lin and Y. H. Zhou: *J. Mater. Sci. Lett.*, 1996, **15**, 2112–2114.
28. K. Zhang and G. N. Chen: *Mater. Sci. Technol.*, 2001, **17**, (6), 668–670.
29. D. W. Tang, B. L. Zhou, H. Cao and G. H. He: *Appl. Phys. Lett.*, 1991, **59**, (24), 3113–3114.
30. D. W. Tang, B. L. Zhou, H. Cao and G. H. He: *J. Appl. Phys.*, 1993, **73**, (8), 3749–3752.

Key Engineering Materials Vols. 315-316 (2006) pp. 344-347
online at http://www.scientific.net

Selective Laser Sintering of Multi-component Cu-based Alloy for Creating Three-dimensional Metal Parts

D.D. Gu[1,a] and Y.F. Shen[1]

[1]College of Materials Science and Technology, Nanjing University of Aeronautics and Astronautics, Nanjing 210016, China

[a]dongdonggu@hotmail.com

Keywords: Rapid prototyping, Selective laser sintering, Cu-based alloy, Microstructure

Abstract. Selective laser sintering (SLS) of a multi-component Cu-based alloy, which consisted of a mixture of Cu, CuSn, and CuP powder, was successfully processed. The XRD, SEM, and EDX analysis shows that the bonding mechanism of this process is liquid phase sintering with partial melting of the powder occurred. The CuSn powder with lower melting point acts as the binder, while the Cu powder with higher melting point acts as the structural metal. The element phosphorus acts as a fluxing agent to prevent the Cu particles form oxidation. The distribution of phosphorus shows higher concentration at grain boundaries due to low solubility of P in Cu. A case study on SLS of this powder system to fabricate a gear was carried out. The relative density of 82% and radial dimension error of 1.9% were achieved.

Introduction

Selective Laser Sintering (SLS) is a typical Rapid Prototyping (RP) technique which holds the capability of producing three-dimensional (3D) full-density parts directly from powders with minimal or no pre-processing and post-processing requirements [1]. Recent research efforts have demonstrated the great potential to fabricate metal components with controlled microstructures and mechanical properties by SLS process [2]. Metallic SLS has been commercially available to produce high performance engineering parts such as functional prototypes and low-volume tools for injection molding and die casting [3].

Copper and copper alloys are widely used materials owing to their excellent thermal and electrical conductivities, ease of material processing, and low cost [4], which also makes them particularly suitable for SLS. The Cu-based powder systems that have been investigated include: CuSn [5], CuSn-Ni [6] and Cu-SCuP [4]. However, till now, common problems associated with metallic SLS such as "balling" effect, curling deformation, low sintered density, weak strength, and high surface roughness are still difficult to completely overcome. This might be caused by the complex nature of SLS, in which multiple modes of heat and mass transfer, and in some instances, chemical reactions may occur [2]. In fact, the SLS of metal powder is still in its early stage of development. Significant research efforts are still required to study the basic principles of SLS process, especially the bonding mechanism of metal powder during laser sintering [7].

This paper reports the results of an investigation into direct SLS of a special multi-component Cu-based metal powder. The phase transformation and microstructural evolution of this powder system during SLS are addressed, with an overall aim to assess its laser sintering behavior.

Experimental Procedure

Powder Preparation. Electrolytic 99% Cu powder with irregular structure and mean equivalent spherical diameter of 54μm, water-atomized CuSn (10 wt. % Sn) powder with ellipsoidal shape and particle size distribution of 11-46μm, and gas-atomized CuP (8.4 wt. % P) powder with spherical morphology and particle size ranging from 5 to 24μm were used in this experiment. Phosphorus, taking as a fluxing agent, was added as pre-alloyed CuP to improve the wetting characteristics in the